Lifetimes of the lowest $\frac{5}{2}^+$ and $\frac{9}{2}^+$ states in the mirror nuclei ^{23}Na-^{23}Mg

P. Tikkanen, J. Keinonen, K. Arstila, and A. Kuronen
Accelerator Laboratory, University of Helsinki, Hämeentie 100, SF-00550 Helsinki, Finland

B. H. Wildenthal
Department of Physics and Astronomy, University of New Mexico, Albuquerque, New Mexico 87131
(Received 13 February 1990)

Mean lifetimes of the first $\frac{5}{2}^+$ and $\frac{9}{2}^+$ states in the mirror nuclei ^{23}Na-^{23}Mg have been measured by application of the Doppler-shift attenuation method and the reactions ^{12}C(^{12}C,p)^{23}Na, ^{12}C(^{15}N,α)^{23}Na, and ^{12}C(^{12}C,n)^{23}Mg. The results are 1800±110 and 1570±170 fs ($\frac{5}{2}^+$), and 139±10 and 91±12 fs ($\frac{9}{2}^+$) for ^{23}Na and ^{23}Mg, respectively. For the effective stopping of recoils, the targets were prepared by implanting ^{12}C into Ta backings. The Monte Carlo method and experimentally confirmed electronic and nuclear stopping powers were used in the Doppler-shift attenuation analysis. The experimental transition strengths are compared with the predictions of recent shell-model calculations.

I. INTRODUCTION

The strong rotational collectivity in nuclei of the light *sd*-shell region has very recently been discussed in the frame work of shell-model wave functions,[1] a shell-model realization of the triaxial quantum rotor,[2] and Nilsson-Strutinsky cranking formalism.[3] The most sensitive test for the description of the microscopic structure of the $K^\pi=\frac{3}{2}^+$ ground-state band in ^{23}Na,[1] was the electric quadrupole ($E2$) matrix elements calculated from the lifetimes of the excited states. In the deduction of the prolate deformation of the $K^\pi=\frac{3}{2}^+$ intrinsic state in ^{23}Na,[1] the total $E2$ proton transition matrix element $M(E2)_p=[(2J_i+1)B(E2)]^{1/2}$ which corresponds to experimentally obtained $B(E2)$ values of in-band transitions was compared with the renormalized model-space proton-neutron matrix elements $A(E2)_{p/n}$

$$M(E2)_p=\tilde{e}_p A(E2)_p+\tilde{e}_n A(E2)_n \ . \quad (1)$$

The effective charges $\tilde{e}_p$ and $\tilde{e}_n$ take into account the effects of model-space truncations. The values have been obtained from a fit of theoretical $E2$ strengths with experimental data in the whole *sd*-shell region.[4]

The low-lying $\frac{5}{2}^+$, $\frac{7}{2}^+$, and $\frac{9}{2}^+$ levels of the $K^\pi=\frac{3}{2}^+$ ground-state band have been identified in the mirror nuclei ^{23}Na-^{23}Mg (Refs. 5 and 6). Previous to this experiment several studies have been reported in the literature on the lifetime values of the lowest $\frac{5}{2}^+$, $\frac{7}{2}^+$, and $\frac{9}{2}^+$ states in ^{23}Na (Ref. 6). The main part of the results have been obtained in Doppler-shift attenuation (DSA) measurements. Lifetimes of the analogue states in the mirror nucleus ^{23}Mg have been obtained in only two DSA measurements.[6] Due to the different slowing-down conditions and in most cases the use of the slowing-down theory[7] without sufficient experimental confirmation, the reported values have large uncertainties and mutual inconsistencies.

This paper describes lifetime measurements of the mirror $\frac{5}{2}^+$ and $\frac{9}{2}^+$ states using the improved DSA method as developed in our laboratory.[8–10] This work is a continuation of our recent study on short lifetimes in ^{24}Mg for test of rotational collectivity in shell-model wave functions.[10] The motivation of this paper was to study the collectivity in the lower part of the *sd*-shell by utilizing the mirror $E2$ transitions in ^{23}Na and ^{23}Mg.

II. EXPERIMENTAL ARRANGEMENTS

The 5-MV tandem accelerator EGP-10-II of the laboratory supplied the 15–24-MeV $^{12}C^{q+}$ ($q=2,3$) beams of about 300 nA and 15–27 MeV $^{15}N^{q+}$ ($q=3-5$) beams of about 400 nA. The beams were collimated to form a spot of 2×2 mm^2 on the target.

The ^{12}C targets were prepared by implanting a 14-μg/cm^2 fluence of 100 keV $^{12}C^+$ ions into 0.4-mm thick tantalum backings at the isotope separator of the laboratory.

The γ radiation was detected in a PGT 120 cm^3 and Canberra 83.4 cm^3 Ge(Li) detector with efficiencies of 28 and 18%, respectively. The energy resolutions of the detection systems were 2.3 and 2.2 keV at $E_\gamma=1.33$ MeV and 3.2 and 3.1 keV at $E_\gamma=2.6$ MeV, respectively. In the $n\gamma$-coincidence measurements neutrons were detected in a 10×5 (diameter) cm liquid scintillator NE213 connected to a fast photomultiplier tube. Neutron and γ-ray initiated pulses were discriminated by utilizing their different scintillation decay times.[8] Furthermore, a 0.7-cm thick lead absorber was used to reduce the γ-counting rate. The detection threshold for neutrons was set by using the Compton edge of the ^{60}Co γ rays. In the $p\gamma$-coincidence measurements protons were detected in a 50-mm^2 Si(Au) surface barrier detector.

The singles, neutron-gated or proton-gated spectra were stored in the 4K or 8K memories of the PDP 11/44 computer. The dispersions were 0.25–1.0 keV/channel.

 ©1990 The American Physical Society

The stability of the spectrometer was checked with a ^{208}Tl γ source and ^{40}K laboratory background. The energy and efficiency calibration of the γ detectors was done with a ^{56}Co source placed in the target position.[11]

III. MEASUREMENTS AND RESULTS

The population of excited nuclear levels in ^{23}Na and ^{23}Mg and the recoil velocities of these atoms were obtained through the reactions ^{12}C(^{12}C,p)^{23}Na, ^{12}C(^{15}N,α)^{23}Na, and ^{12}C(^{12}C,n)^{23}Mg. A summary of the measurements is given in Table I.

The Doppler shifted γ rays were detected at the angle 0° relative to the beam direction. The detector was located 4.0 cm from the target and was shielded from low-energy γ rays and x rays by 4 mm of lead. The corrections for solid-angle attenuation of the observed Doppler shifts and for the finite initial velocity distribution were determined from fully shifted γ rays of short-lived states using a porous carbon target with very low stopping power.[8] The neutron detector was located at 120° to the beam and at a distance of 5.0 cm from the target. The proton detector was located at 140° to the beam and at a distance of 4.0 cm from the target.

In addition to the line shape, lifetimes were deduced by comparing the attenuated shift with the experimental full shift obtained using the porous carbon target on the Ta backing. The density of the target was 0.09 g cm^{-3} (Ref. 8). By the use of this target and the method described in Ref. 8, the recoil velocities $\beta=2.6-3.5$ % were obtained for ^{23}Na and ^{23}Mg within ± 2% accuracy with the values calculated from the reaction kinematics. In deducing the β value for ^{23}Na and ^{23}Mg, the small correction due to the slowing down in the target was taken into account.

A summary of the results of the DSA measurements is given in Table I. In the deduction of the lifetime values from the line shapes and from the $F(\tau)$ values ($\frac{5}{2}^+$ states) or $1-F(\tau)$ values ($\frac{9}{2}^+$ states), the corrections for the indirect feedings were introduced. The effect of the indirect feedings was studied by using different bombarding energies in the DSA measurements. By comparing the intensity of the feeding transitions with the intensity of the deexciting transitions, the intensity of the prompt feeding was found for each level. The γ-ray decay schemes of the bound states were taken from Ref. 6.

In the analysis of the ^{12}C(^{12}C,p)^{23}Na reaction data the lifetime value of the 0.44-MeV state was corrected at the 16- and 24-MeV bombarding energies for the (relative to the intensity of the 440-keV γ rays) 9% and 20% delayed feedings, respectively, through the cascade 2.70 MeV ($\tau=139$ fs)$\rightarrow$2.08($\tau=40$ fs, Ref. 6)$\rightarrow$0.44 MeV; 18% and 40% feedings, respectively, through the cascade 2.70 MeV$\rightarrow$0.44 MeV; and 22% and 40% feedings, respectively, through the cascade 2.08 MeV$\rightarrow$0.44 MeV. In the analysis of the ^{12}C(^{15}N,α)^{23}Na reaction data the feedings were 9%, 16%, 20%, and 20% (2.70 MeV$\rightarrow$2.08 MeV$\rightarrow$0.44 MeV); 18%, 32%, 40%, and 40% (2.70 MeV$\rightarrow$0.44 MeV); and 31%, 45%, 36%, and 27% (2.70 MeV$\rightarrow$0.44 MeV) at the 15-, 20-, 23-, and 27-MeV bombarding energies, respectively. No correction for delayed feeding was necessary in the lifetime analysis of the 2.70-MeV state. At the 15-, 16-, 18-, and 22.5-MeV bombarding energies of the reaction ^{12}C(^{12}C,n)^{23}Mg the lifetime

TABLE I. Summary of the lifetimes in ^{23}Na-^{23}Mg obtained in this paper.

Nucleus	Reaction	E_{bomb} (MeV)	τ(fs)[a] $\frac{5}{2}^+$	$\frac{9}{2}^+$
^{23}Na	^{12}C(^{12}C,p)	15[b]		136±5
		16[b,c]	1750±250	
		18[b]		142±5
		24[d]	1850±200	143±17
	^{12}C(^{15}N,α)	15[b]	1750±140	
		20[b]	1820±160	
		23[b]	1870±150	
		27[b]	1770±120	
		Adopted	1800±110	139±10
^{23}Mg	^{12}C(^{12}C,n)	15[b]	1680±180	80±20
		16[b,c]	1410±190	90±20
		18[b]	1600±200	90±22
		22.5[e]	1570±180	120±30
		Adopted	1570±120	91±12

[a]The error limits given for the lifetime values from different measurements include the statistical errors and the uncertainties due to the feeding transitions. The values given are adopted from the line shape and centroid shift analysis. The adopted values include also the uncertainties due to the stopping power.
[b] Singles measurement.
[c]The DSA measurement was done at 140° and the detector was located 6.0 cm from the target.
[d]$p\gamma$-coincidence measurement.
[e]$n\gamma$-coincidence measurement.

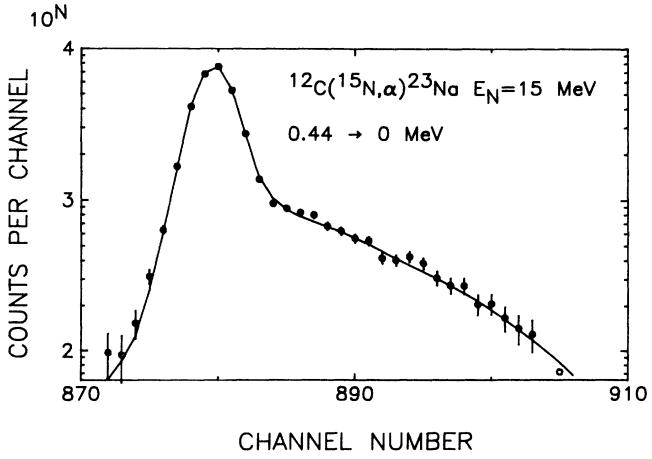

FIG. 1. Portion of γ-ray spectrum recorded in the DSA measurements of the ^{23}Na 0.44$\rightarrow$0 MeV transition observed in the ^{12}C(^{15}N,α)^{23}Na reaction. The dispersion is 0.50 keV/channel. The solid line is the Monte Carlo simulation of the γ-ray line shape at 0°; the fit is for the lifetime 1750 fs. The adopted lifetime including the feeding correction is $\tau(0.44)=1800\pm110$ fs.

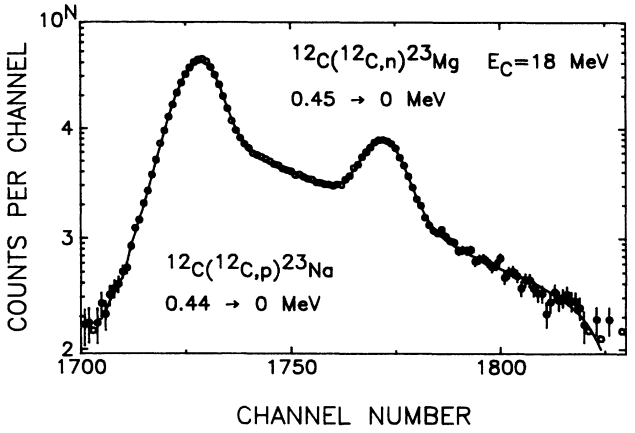

FIG. 2. Portion of γ-ray spectrum recorded in the DSA measurements of the ^{23}Mg 0.45→0 MeV transition observed in the single measurements through the reaction $^{12}C(^{12}C,n)^{23}Mg$. The dispersion is 0.25 keV/channel. The solid line is the Monte Carlo simulation of the γ-ray line shape at 0°; the fit is for the lifetime 1600 fs of the 0.45→0 MeV ^{23}Mg line, and 1800 fs of the 0.44→0 MeV ^{23}Na line. The adopted lifetime including the feeding correction is $\tau(0.45)=1570\pm120$ fs. The fit of the flight part of the 0.44→0 MeV ^{23}Na line with the known lifetime indicated that the intensity in the stop peak from $^{23}Mg(\beta^+)^{23}Na$ was about 2% of the total intensity.

value of the 0.45-MeV state was corrected for the 7%, 7%, 17%, and 10% feedings, respectively, through the cascade 2.72 MeV (τ=91 fs)→2.05 MeV (τ=80 fs, Ref. 6)→0.45 MeV; 14%, 14%, 34%, and 20% feedings, respectively, through the cascade 2.72 MeV→0.45 MeV; and 17%, 26%, 41%, and 24% feedings, respectively, through the cascade 2.05 MeV→0.45 MeV. No correction for delayed feeding was necessary in the DSA analysis of the 2.72-MeV state. The relative uncertainty of the feeding intensities was in all cases taken to be ±30% and was included in the error limits of the deduced lifetime values.

Figures 1–3 show portions of the γ-ray spectra

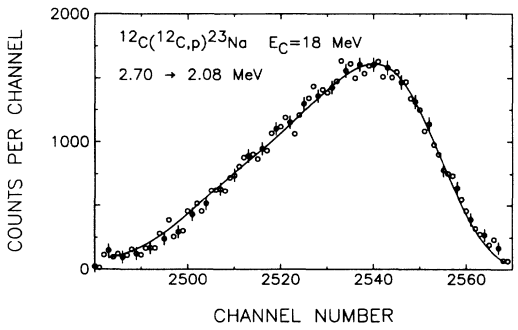

FIG. 3. As for Fig. 2, but for the 2.70-MeV state. The Monte Carlo simulation is for the lifetime 140 fs; $\tau(2.70)=139\pm10$ fs.

from the DSA measurements. Due to the uncertainty caused by the unshifted 440-keV γ rays following $^{23}Mg(\beta^+)^{23}Na$, the lifetime value of the $\frac{5}{2}^+$ state in ^{23}Na was obtained from the reaction $^{12}C(^{15}N,\alpha)^{23}Na$ measurements where ^{23}Mg is not produced and from the $p\gamma$-coincidence measurements with the reaction $^{12}C(^{12}C,p)^{23}Na$.

The DSA analysis was performed using Monte Carlo calculations.[8–10] The stopping power of Ta for ^{23}Mg and

TABLE II. Lifetime measurements of the 0.44-, 2.08-, and 2.70-MeV levels in ^{23}Na.

E_x (MeV)	Method	τ(fs)[a]	Reference
0.44	Res. fluor.	1800±350	16
		1500±250	17
		1800±280	18
		1300±300	19
		1620±100	20
	DSA	1690±220	21
		1630±200	5
		1400±300	22
		1800±110	This work
2.08	Res. fluor.	45±9	23
	Coul. excit.	49±11	24
		50±20	21
	Elect. scat.	46±8	25
	DSA	120±60	21
		38±5[c]	26
		37±9	22
		28.6±3.0[b]	27
		210±60	28
		43±7[b]	29
		50±15 (18)	30
		41.7±3.2	12
		35±4[d]	31
2.70	DSA	110±20	5
		105±20	22
		200±100	32
		100±60	33
		100±25	28
		102±25[b]	29
		125±30(39)	30
		131±18	12
		139±10	This work

[a]The error limits given in the parentheses are deduced by us by adding an uncertainty of 20% in quadrature to the value given by the authors, see the text.
[b]For the reanalyzed value, see Ref. 12.
[c]Value obtained with Ta backing has been reanalyzed and is given here.
[d]Statistical error limits ±3 fs given by the authors have been increased to include the uncertainty ±7% due to the experimental stopping power used by them.

^{23}Na ions was described by

$$\left[\frac{dE}{dx}\right]_{\text{corr}} = (0.70\pm0.05)\left[\frac{dE}{dx}\right]_n + \left[\frac{dE}{dx}\right]_e^{\text{exp}} . \quad (2)$$

The uncorrected nuclear stopping power was calculated by the Monte Carlo method, where the scattering angles of the recoiling ions were directly derived from the classical scattering integral and the interatomic interaction was described by the Thomas-Fermi potential.[9] The relevant data for the description of the nuclear stopping of the recoiling ^{23}Na, and ^{23}Mg nuclei in Ta were taken from our earlier study[12,13] in which the experimental correction parameter for the nuclear stopping power was determined for ^{23}Na recoiling in Ta. Our previous studies[9] indicate that there are no abrupt changes in the stopping power for recoiling atoms with similar Z values. Hence the same correction factor was applied also for ^{23}Mg. The electronic stopping power was obtained by using the recent experimental energy loss values of Ta for ^{26}Mg ions[14] corrected for the ^{23}Na and ^{23}Mg ions in the framework of the semiempirical model by Ziegler *et al.*[15] The absolute uncertainty of the electronic stopping power is ±5%.

The effect of implanted ^{12}C on the density of the backing material and lifetimes obtained by DSA has recently been studied by us.[8,9] The data indicate that at concentrations below about 20 at.% of light implants, possible density changes in Ta have an insignificant effect on the lifetime values. In this paper the maximum concentration was about 10 at.% determined by backscattering of 12 MeV ^{14}N particles.

The lifetimes of the lowest $\frac{5}{2}^+$, $\frac{7}{2}^+$, and $\frac{9}{2}^+$ states in ^{23}Na have been measured several times by several independent methods. The previous results along with our measurements for the $\frac{5}{2}^+$ and $\frac{9}{2}^+$ states are summarized in Tables II and III and displayed in Figs. 4 and 5. In the cases of the $\frac{7}{2}^+$ states, the values of the considerably shorter lifetimes than the lifetimes of the feeding $\frac{9}{2}^+$ states were obtained to depend so strongly on the ratio of the delayed to prompt feeding intensity that within the uncertainties it was not meaningful to compare the present values with the previous ones. In the figures the values of the weight of the measurements, on a logarithmic scale, are plotted as function of the lifetime values. The weight is assumed to be $(\Delta\tau)^{-2}$ where $\Delta\tau$ is the quoted uncertainty of the lifetime measurement. The reference value is the adopted value and contours at $\pm2(\Delta\tau)$ are centered at this value. In those few cases where only a statistical error has been reported in the literature or where no information is available on the DSA analysis, an uncertainty of 20% has been added in quadrature for the comparison with the values from those measurements for which the uncertainty due to the stopping power is included (see Table II). Note that in the cases where the literature data include such an uncertainty, the values obtained without the experimental stopping data are still subject to a systematic error. The experimental conditions of the present and previous DSA measurements are shown in Table IV. All previous studies used nuclear

TABLE III. Lifetime measurements of the 0.45-, 2.05,- and 2.72-MeV levels in ^{23}Mg.

E_x (MeV)	Method	τ(fs)	Reference
0.45	DSA	1650±250	34
		$3600\pm^{9000}_{2400}$	35
		2000±240	5
		1570±120	This work
2.05	DSA	80±20	34
2.72	DSA	140±30	34
		80±20	5
		91±12	This work

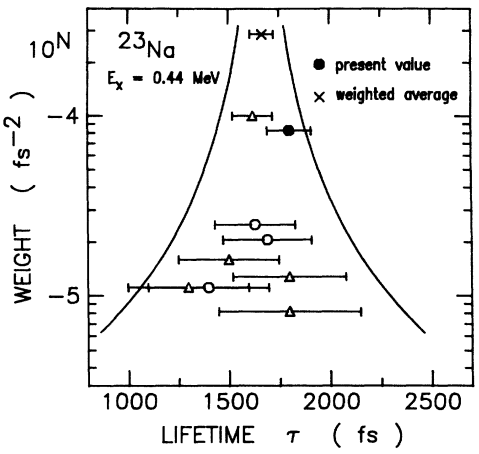

FIG. 4. A plot of the weights of lifetime measurements of the ^{23}Na 0.44-MeV state versus lifetime values. The weight of a measurement is taken as $(\Delta\tau)^{-2}$ where $\Delta\tau$ is the quoted uncertainty. The values are from Table II. The data from DSA measurements are shown by circles and those from resonance fluorescence measurements by triangles. Two contours of τ(adopted)$\pm2(\Delta\tau)$ are also shown.

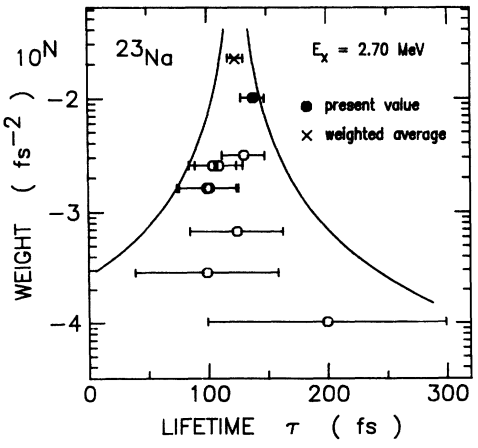

FIG. 5. As for Fig. 4, but for the 2.70-MeV state.

stopping powers obtained from the LSS theory[7] with the large-angle scattering correction as given by Blaugrund.[36] The use of the Blaugrund approximation instead of the realistic Monte Carlo method in calculation of the attenuation factor, would make the present lifetime values of the $\frac{5}{2}^+$ states shorter by a factor of about 0.9. It is worth noting that in spite of the fact that the recoiling nuclei are in some previous experiments produced in the

TABLE IV. Summary of DSA measurements of lifetimes in ^{23}Na-^{23}Mg. If the stopping powers from the LSS theory (Ref. 7) with the large-angle scattering corrections by Blaugrund (Ref. 36) have not been used in the DSA analysis, it is marked in the footnotes.

	Work	Reaction	v/c (%)	Slowing-down medium	DSA analysis
^{23}Na:	Present	^{12}C(^{15}N,α)	2.6–3.5	Ta and implanted ^{12}C	a
	Present	^{12}C(^{12}C,p)	2.6–3.3	Ta and implanted ^{12}C	a
	5		2.9	50 μg/cm^2 C on a thick Al backing	b
				100 μg/cm^2 C on a thick Ni backing	b
	30		3.5	80 μg/cm^2 C on a 0.125-mm Au backing	c
	20	^{23}Na(^{35}Cl,^{35}Cl′)	<7	Na	d
	20	^{23}Na(^{32}S,^{32}S′)	<7	NaCl	d
	22	^{20}Ne(α,p)	1.6–1.7	Ta and implanted ^{20}Ne	e
	26	^{22}Ne(p,γ)	0.2	Ta and implanted ^{22}Ne	
	27		0.2	Mo or Ta and implanted ^{22}Ne	f
	29		0.2	Ta and implanted ^{22}Ne	g
	12		0.2	Ta and implanted ^{22}Ne	a
	31		0.2	Ta and implanted ^{22}Ne	a
	28	^{23}Na(p,$p'\gamma$)	0.4–0.5	Metallic, 1.0–1.3 mg/cm^2 Na on Au	h
	32		0.4–0.5	Metallic ^{23}Na on NaI	i
	33		0.4–0.5	2 mg/cm^2 on NaOH on Ta backing	j
^{23}Mg:	Present	^{12}C(^{12}C,n)	2.6–3.2	Ta and implanted ^{12}C	a
	21		2.9	50 μg/cm^2 C on a thick Al backing	b
				100 μg/cm^2 C on a thick Ni backing	b
	34	^{24}Mg(τ,α)	1.1–1.3	150 μg/cm^2 Mg on 200 μg/cm^2 C	k
	35	^{23}Na(p,n)	0.5	9 mg/cm^2 NaCl on thick Au backing	l

[a]Experimental stopping power. Monte Carlo simulation of the slowing down.

[b]The energy loss parametrized by the equation

$$\frac{dE}{dx}=K_n\left[\frac{v}{v_0}\right]^{-1}+K_e\left[\frac{v}{v_0}\right]-K_3\left[\frac{v}{v_0}\right]^3,$$

where $v_0=c/137$ and K_n, K_e, and K_3 are parameters obtained by fitting this equation with experimental electronic stopping data. K_n according to the LSS theory (Ref. 7) and the large-angle scattering by Blaugrund (Ref. 36).

[c]The electronic stopping power from the compilation of Northcliffe and Schilling (Ref. 37).

[d]The energy loss parametrization as in footnote b for low velocities. For high velocities the energy loss was parametrized using

$$\frac{dE}{dx}=A+B\left[\frac{v}{v_0}\right]+C\left[\frac{v}{v_0}\right]^2,$$

where A, B, and C were obtained by fitting this equation with experimental data.

[e]In addition to the statistical errors a 20% uncertainty of the stopping power was included in the reported values.

[f]The stopping power from the LSS theory (Ref. 7) corrected by a factor of 1.16. For the reanalyzed values, see Ref. 12.

[g]The electronic stopping power from the LSS theory was corrected by the data from Ref. 38. The data have been reanalyzed in Ref. 12.

[h]In addition to the statistical errors a 25% uncertainty of the stopping power was included.

[i]Electronic stopping power from the LSS theory (Ref. 7) reduced by 18±10% according to the systematics from Ref. 38. The parametrization of the stopping power according to Ref. 5, see footnote b.

[j]Stopping power from the LSS theory (Ref. 7) with the large-angle scattering by Blaugrund (Ref. 36) was used for slowing down in Ta. Electronic stopping power of NaOH from the LSS theory was corrected for by the systematic periodical deviations according to the data in Ref 39. The uncertainty in the stopping powers was evaluated to be ±10%.

[k]The electronic stopping power from the LSS theory (Ref. 7) was corrected with the experiments by Ormrod *et al.* (Ref. 38) and Fastrup *et al.* (Ref. 40). Uncertainty in the electronic stopping power was estimated to amount to 20%.

[l]The $F(\tau)$ curve calculated with the stopping power from the LSS theory (Ref. 7) and the large-angle scattering by Blaugrund (Ref. 38) was corrected so that the simultaneously measured lifetime of the 0.44-MeV state in ^{23}Na was renormalized to be 1600±80 fs.

velocity region where the electronic stopping power is dominant (as in this paper) the line shape corresponding to the long lifetime is strongly affected by the large angle scattering. This could be circumvented in the line-shape analysis by fitting only that part of the line shape which corresponds to known stopping power and where the effect of nuclear scattering is negligibly small. This procedure has been shown to yield consistent lifetime values in high-velocity DSA measurements.[21,41] However, this method has been applied to ^{23}Na only in Ref. 21. In previous studies the electronic stopping powers were taken from the LSS[7] theory or were based on experimental data or systematics of experimental data.

IV. DISCUSSION

Electromagnetic matrix elements for transitions between low-lying states of ^{23}Na and ^{23}Mg are deduced from the lifetimes of the decaying states (as measured in the present experiments and combined with previous results as described above) and the branching and mixing ratios tabulated in Ref. 6. These experimental matrix element values are presented in Table V in comparison with theoretical values calculated from the full-*sd*-shell wave functions of the USD Hamiltonian.[42]

The USD wave functions have been shown to yield a generally good accounting for spectroscopic features of *sd*-shell states when combined with the appropriate effective operators. The $E2$ and $M1$ operators used to calculate the matrix elements listed in Table V have been obtained from analyses of a compilation[43] of electromagnetic data for states of $A=17-39$ nuclei. In these analyses, the one-body densities calculated from the USD wave functions are matched with the corresponding experimental matrix elements and the optimal corrections to the conventional free-nucleon parametrizations of the $E2$ and $M1$ operators are extracted by least-squares fits.

The $E2$ effective operator was determined[4] in the context of a model in which the neutrons and protons are assumed to carry orbital and state-independent effective charges. The single-particle wave functions are assumed to have harmonic oscillator radial dependence and a mass dependence of the form $\hbar\omega=45\ A^{-1/3}-25\ A^{-2/3}$. The $M1$ effective operator was determined[44] in the context of a model in which the orbital, spin ($l=2$ and $l=0$ components treated independently), and tensor terms of the operator were allowed to have correction terms determined from the fit. The rationale for using effective operators of this sort, "renormalizations" of the values obtained by using the free-space values of the neutron and proton charges and moments, is the need to compensate for nuclear configurations and nucleonic states which are excluded from the model space in which the wave functions are generated. The correction values obtained empirically, as described above, are consistent with values obtained from theoretical studies.[45] A smooth mass-dependence of the form $\delta(A)=\delta(A=28)\times(A/28)^{0.35}$ of the effective charges and moments was assumed.

TABLE V. Absolute values of experimental and theoretical transition matrix elements[a] in ^{23}Na-^{23}Mg.

E_i (MeV)	E_f (MeV)	J_i^π	J_f^π	τ (fs)	Branching (%)	$M1$ matrix element (μ_N)[b] Expt.	*SM*	$E2$ matrix element ($e$fm^2)[b] Expt.	*SM*
					^{23}Na				
0.44	0	$\frac{5}{2}^+$	$\frac{3}{2}^+$	1660±60	100	1.55±0.06[c]	1.45	24.6±1.5[c]	25.2
2.08	0	$\frac{7}{2}^+$	$\frac{3}{2}^+$	37±2	9.0±1.0			20±2	17.6
	0.44		$\frac{5}{2}^+$		91.0±1.0	1.58±0.04[d]	1.41	21±2[d]	21.8
2.70	0.44	$\frac{9}{2}^+$	$\frac{5}{2}^+$	125±7	64.0±1.0			26.5±0.9	23.6
	2.08		$\frac{7}{2}^+$		36.0±1.0	2.57±0.09[e]	2.17	39±10[e]	20.5
					^{23}Mg				
0.45	0	$\frac{5}{2}^+$	$\frac{3}{2}^+$	1660±110	100	1.50±0.07[f]	1.33	24±8[f]	25.8
2.05	0	$\frac{7}{2}^+$	$\frac{3}{2}^+$	80±20	16±2			20±3	18.9
	0.45		$\frac{5}{2}^+$		84±2	1.06±0.13[g]	1.28	15±2[g]	22.7
2.72	0.45	$\frac{9}{2}^+$	$\frac{5}{2}^+$	94±12	68±2			31±4	26.1
	2.05		$\frac{7}{2}^+$		32±2	<3.4	2.29	<510	20.1

[a]Except for lifetimes, the values are taken from Ref. 6.
[b]If the mixing ratios are not known, the experimental matrix elements are given for pure multipoles.
[c]$\delta(E2/M1)=-0.058\pm0.003$.
[d]$\delta(E2/M1)=-0.19\pm0.02$.
[e]$\delta(E2/M1)=-0.08\pm0.02$.
[f]$\delta(E2/M1)=0.06\pm0.02$.
[g]$\delta(E2/M1)=0.19\pm0.02$.

The data set[42] used for determining the $E2$ effective operator consisted of the 147 experimental matrix elements from *sd*-shell transitions which have uncertainties of $\pm 10\%$ or less. The effective charges extracted from the fit to these data were $+0.389e$ for the isoscalar charge $[(\delta e_p + \delta e_n)/2]$ and $-0.089e$ for the isovector charge $[(\delta e_p - \delta e_n)/2]$. The corresponding effective charges are $\tilde{e}_p = 1.300e$ and $\tilde{e}_n = 0.478e$. The data set used for determining the $M1$ effective operator consisted of matrix elements obtained from both magnetic moments and $M1$ transitions. Again, only values with uncertainties smaller than $\pm 10\%$ were included. The parametrization of the effective $M1$ operator and the resulting values for the renormalization are discussed in detail in Ref. 44. Theoretical values of $M1$ and $E2$ matrix elements for ^{23}Na and ^{23}Mg transitions were then calculated with these effective operators and are listed in Table V. Within the experimental uncertainties the agreement between the experimental and theoretical values is very good. The largest deviations can be seen in those cases where the large uncertainties of the mixing ratios results in the large uncertainties of the $E2$ matric elments.

ACKNOWLEDGMENTS

This work was supported by the Academy of Finland.

[1]M. Carchidi and B. H. Wildenthal, Phys. Rev. C **37**, 1 (1988).
[2]J. P. Draayer, S. C. Park, and O. Castanos, Phys. Rev. Lett. **62**, 20 (1989).
[3]R. K. Sheline, I. Ragnarsson, S. Åberg, and A. Watt, J. Phys. G **14**, 1201 (1988).
[4]B. H. Wildenthal, J. Keinonen, and B. A. Brown (unpublished).
[5]E. K. Warburton, J. J. Kolata, and J. W. Olness, Phys. Rev. C **8**, 1385 (1973).
[6]P. M. Endt and C. van der Leun, Nucl. Phys. **A310**, 1 (1978).
[7]J. Lindhard, M. Scharff, and H. E. Schiøtt, Mat. Fys. Medd. Dan. Vid. Selsk. **33**, No. 14 (1963).
[8]P. Tikkanen, J. Keinonen, V. Karttunen, and A. Kuronen, Nucl. Phys. **A456**, 337 (1986).
[9]J. Keinonen, in *Capture γ-Ray Spectroscopy and Related Topics-1984*, edited by S. Raman (AIP, New York, 1985), p. 557.
[10]J. Keinonen, P. Tikkanen, A. Kuronen, Á. Z. Kiss, E. Somorjai, and B. H. Wildenthal, Nucl. Phys. **A493**, 124 (1989).
[11]M. Hautala, A. Anttila, and J. Keinonen, Nucl. Instrum. Methods **150**, 599 (1978).
[12]A. Anttila, M. Bister, and J. Keinonen, Z. Phys. **A274**, 227 (1975).
[13]A. Luukkainen, J. Keinonen, and M. Erola, Phys. Rev. B **32**, 4814 (1985).
[14]K. Arstila, J. Keinonen, and P. Tikkanen, Phys. Rev. B **41**, 6117 (1990).
[15]J. F. Ziegler, J. P. Biersack, and U. Littmark, in *The Stopping and Range of Ions in Solids*, edited by J. F. Ziegler (Pergamon, New York, 1985), Vol. 1.
[16]V. K. Rassmussen, F. R. Metzger, and C. P. Swann, Nucl. Phys. **13**, 95 (1959).
[17]B. Ambrozy, A. Faudrowicz, A. Jasinski, J. Kownacki, H. Lancman, and J. Ludziejewski, Acta Phys. Pol. **20**, 537 (1961).
[18]W. L. Mouton, J. P. F. Sellschop, and R. J. Keddy, Phys. Rev. **128**, 2745 (1962).
[19]C. P. Swann, Nucl. Phys. **42**, 602 (1963).
[20]S. J. Skorka, D. Evers, J. Hertel, J. Morgenstein, T. W. Retz-Schmidt, and H. Schmidt, Nucl. Phys. **81**, 370 (1966).
[21]D. Schwalm, E. K. Warburton, and J. W. Olness, Nucl. Phys. **A293**, 425 (1977).
[22]H. Grawe, K. Holzer, K. Kaendler, and A. A. Pilt, Nucl. Phys. **A237**, 18 (1975).
[23]V. K. Rasmussen, Nucl. Phys. **A169**, 166 (1971).
[24]O. F. Afonin, A. P. Grinberg, I. Kh. Lemberg, and I. N. Chugumov, Yad. Fiz. **6**, 219 (1966) [Sov. J. Nucl. Phys. **6**, 160 (1967)].
[25]G. A. Sawitskin, N. G. Afanasev, I. S. Gulkarov, V. D. Kovalev, V. M. Khvastunov, N. G. Shechenko, and I. V. Andreeva, Izv. Akad. Nauk. Ser. Fiz. **33**, 60 (1969).
[26]M. Bister, A. Anttila, and M. Piiparinen, Ann. Acad. Sci. Fennicae Ser. **AVI**, No. 349 (1970).
[27]Z. B. Du Toit, P. R. De Kock, and W. L. Mouton, Z. Phys. **246**, 170 (1971).
[28]J. L. Durell, P. R. Alderson, D. C. Bailey, L. L. Green, M. W. Greene, A. N. James, and J. F. Sharpey-Schafer, J. Phys. A **5**, 302 (1972).
[29]M. A. Meyer and J. J. A. Smit, Nucl. Phys. **A205**, 177 (1973).
[30]G. G. Frank, R. V. Elliot, R. H. Spear, and J. A. Kuehner, Can. J. Phys. **51**, 1155 (1973).
[31]J. J. A. Smith, M. A. Meyer, J. P. L. Reinecke, and D. Reitmann, Nucl. Phys. **A318**, 111 (1979).
[32]A. R. Poletti, A. D. W. James, J. A. Becker, R. E. McDonald, and R. W. Nightingale, Phys. Rev. **184**, 1130 (1969).
[33]H. J. Maier, J. G. Pronko, and C. Rolfs, Nucl. Phys. **A146**, 99 (1970).
[34]R. Engmann, F. Brandolini, and I. Mauritzson, Nucl. Phys. **A171**, 418 (1971).
[35]T. Itahashi, T. Shibata, and T. Wakatsuki, J. Phys. Soc. Jpn. **31**, 961 (1971).
[36]A. E. Blaugrund, Nucl. Phys. **88**, 501 (1966).
[37]L. C. Northcliffe and R. F. Schilling, Nucl. Data **A7**, 233 (1970).
[38]J. H. Ormrod, J. R. McDonald, and H. E. Duckworth, Can. J. Phys. **43**, 275 (1965).
[39]L. C. Northcliffe, Annu. Rev. Nucl. Sci. **13**, 67 (1963).
[40]B. Fastrup, P. Hvelplund, and C. A. Sautter, Mat. Fys. Medd. Dan. Vid. Selsk. **35**, No. 10 (1966).
[41]J. S. Forster, T. K. Alexander, G. C. Ball, W. G. Davies, I. V. Mitchell, and K. B. Winterbon, Nucl. Phys. **A313**, 397 (1979).
[42]B. H. Wildenthal, in *Capture γ-Ray Spectroscopy and Related Topics-1984* (Ref. 9), p. 89.
[43]B. H. Wildenthal and J. Keinonen (unpublished).
[44]B. A. Brown and B. H. Wildenthal, Nucl. Phys. **A474**, 290 (1987).
[45]I. S. Towner, Phys. Rep. **155**, 264 (1987).